

Neutron dosimeters employing high-efficiency perforated semiconductor detectors

Q. Jahan, E. Patterson, B. Rice, W.L. Dunn *, D.S. McGregor

Department of Mechanical and Nuclear Engineering, Kansas State University, 302 Rathbone Hall, Manhattan, KS 66506, United States

Available online 1 May 2007

Abstract

A technology that makes use of recently developed high-efficiency, low-power semiconductor detectors for neutron dosimetry is described. Silicon semiconductor material is perforated using plasma etching techniques; the surface is then coated and the perforations are filled with neutron reactive material. These perforated detectors appear to be capable of greater than 40% efficiency when used in a sandwich design. Devices incorporating bare and cadmium-filtered perforated semiconductor detectors with micro-controller hardware to process and readout the detectors can be made small enough to function as portable neutron dosimeters. Monte Carlo modeling that relates the detector responses to phantom dose equivalent at various positions on an elliptical water phantom is discussed.

© 2007 Elsevier B.V. All rights reserved.

1. Introduction

Semiconductor detectors that incorporate neutron reactive material within the diode substrate offer a promising approach to neutron dosimetry. The reactive materials most often used for neutron detection are either pure ^{10}B or ^6LiF . The particle energies emitted from the $^{10}\text{B}(n, \alpha)^7\text{Li}$ and the $^6\text{Li}(n, \alpha)^3\text{H}$ reactions are relatively large and produce signals easily distinguished from γ -ray background. We are developing semiconductor diode detectors, based on the design first proposed by McGregor et al. [1], that offer thermal neutron detection efficiencies approaching 50%, have low-power consumption and are of modest size. Use of two detectors, one bare and one incorporating a cadmium (Cd) filter, allows measurement of both thermal and epithermal neutrons. Such detectors can be incorporated into a dosimeter package that can measure and display approximate ambient dose equivalents.

The two charged particles from both the ^{10}B and ^6Li absorption reactions are released in opposite directions, if the neutron energy is negligible. The microscopic neutron absorption cross-section of ^{10}B is 3840 b at thermal energy

(0.0253 eV) and decreases with increasing neutron energy as the inverse of the neutron speed ($1/v$) over a significant energy range [2]. A similar situation holds for the cross-section of ^6Li , which is 940 b at thermal energy and varies approximately as $1/v$ except at certain resonances including one at 100 keV, in which the absorption cross-section surpasses that of ^{10}B for energies between approximately 150 keV and 300 keV [2]. Due to its higher thermal absorption cross-section, the $^{10}\text{B}(n, \alpha)^7\text{Li}$ reaction leads to a generally higher reaction probability than the $^6\text{Li}(n, \alpha)^3\text{H}$ reaction for neutron energies below 100 keV. However, the higher-energy reaction products emitted from the $^6\text{Li}(n, \alpha)^3\text{H}$ reaction are easier to detect than the particles emitted from the $^{10}\text{B}(n, \alpha)^7\text{Li}$ reaction.

2. Design

Thermal efficiencies of coated semiconductor detectors traditionally have been limited to less than 5%. However, high-efficiency neutron detectors can be developed by utilizing a cavity structure in which deep trenches are etched into the diode surface and then are filled with neutron reactive material [1]. The design allows for neutron reactive material to cover more surface area of the device and to have a greater probability of ejecting a reaction product

* Corresponding author. Tel.: +1 785 532 5628; fax: +1 785 532 7057.
E-mail address: dunn@mne.ksu.edu (W.L. Dunn).

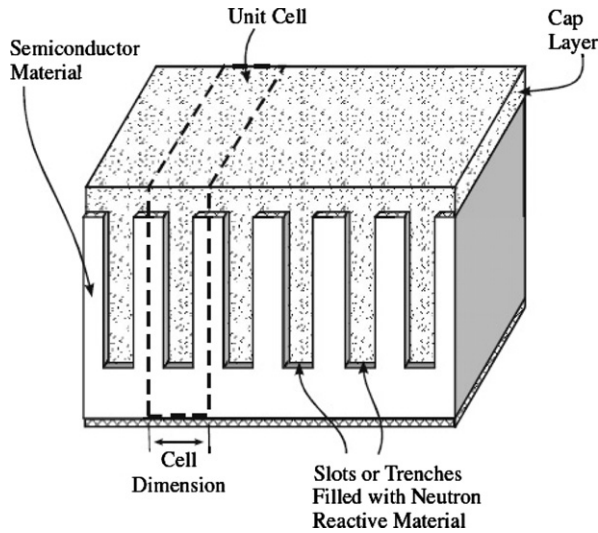


Fig. 1. A semiconductor cavity structure that uses linear-trenches filled with neutron reactive material.

into the semiconductor substrate. Fig. 1 illustrates a linear-trench concept, in which a “unit cell” is defined by the centerlines separating the trenches, which extend through the length and depth of the semiconductor. The “cap thickness” refers to the upper-most ^{10}B or ^6LiF layer covering the device surface. The trenches are interrupted by occasional cross-segments of semiconductor material for mechanical stability. Calculations have demonstrated that thermal neutron detection efficiencies of devices constructed in this manner, in principle, can approach 25%.

If two such devices are combined in a sandwich design, where the trenches in one layer overlap the semiconductor in the other, the intrinsic thermal neutron detection efficiency can exceed 40%. The dosimeters will incorporate two sandwich detectors, one with a Cd filter to eliminate thermal neutrons and one without Cd shielding to accept neutrons at all energies. When constructed from high-purity Si material (float-zone refined), the detectors will require only a modest voltage to operate. The detectors are being integrated into a small package that includes low-power micro-controller hardware, which consists of analog detection and computation components and LED readout. Hence, a battery can be used to operate the detectors and the readout electronics. The package is expected to occupy a volume of only about $2 \times 4 \times 6$ cm. A prototype device has been fabricated and is currently being tested. Here, we report on Monte Carlo simulation studies that relate detector responses to the neutron field.

3. Simulation studies

We consider a 40-cm wide by 70-cm high parallel beam of neutrons incident on an elliptical water phantom of height 70 cm and major- and minor-axis dimensions of 40 cm and 20 cm, respectively. We used the MCNP Monte Carlo simulation code [3] to estimate the responses of

detectors placed in front of the phantom. We normalized our detector responses for a beam that would produce 1 mSv ambient dose equivalent if incident on the ICRU sphere phantom; this is 1/50th of the annual occupational exposure limit suggested by the National Council on Radiation Protection and Measurements [4] for stochastic effects. A neutron beam will produce a dose equivalent in the ICRU sphere given by

$$H = \int_0^{\infty} \Phi(E) \mathfrak{R}_H(E) dE, \quad (1)$$

where $\mathfrak{R}_H(E)$ is the neutron ambient dose equivalent response function, which is given in Table A2.1 of [5] and for the parallel beam

$$\Phi(E) = S_a \chi(E), \quad (2)$$

with S_a the beam intensity per unit area and $\chi(E)$ the probability density function for neutron energy. Thus, $H = S_a I$, where

$$I = \int_0^{\infty} \chi(E) \mathfrak{R}_H(E) dE \quad (3)$$

and, since MCNP scores results per source neutron,

$$S_a = \frac{1}{40(70)} = \frac{1}{2800} \text{ cm}^{-2}. \quad (4)$$

We considered seven cases: a Maxwellian spectrum for neutrons of characteristic energy 0.0253 eV, a Watt fission spectrum typical of ^{235}U and monoenergetic neutrons of 1, 2, 3, 4 and 5 MeV. The appropriate normalization factors for these cases are given in Table 1.

Both the bare and cadmium-filtered detectors were modeled as cylindrical disks of diameter 1 cm and thickness 0.05 mm. The filtered detector had a 30 μm layer of cadmium behind it (between the detector disk and the phantom). We considered, for illustration purposes, only boron-loaded detectors, where, for simplicity, the ^{10}B is assumed uniformly distributed throughout the semiconductor substrate (because in the sandwich design all areas project a boron layer to the incoming neutrons). Each detector is assumed to be 40% efficient. The two detectors are placed as a pair in front of the water phantom and the centers of the two detectors are separated vertically by 2 cm. We placed the pair of detectors on the front surface of the water phantom at each of eight different positions, as shown schematically in Fig. 2. The centers of

Table 1
MCNP normalization factors for the seven neutron source cases considered

Neutron energy case	$\frac{1}{S_a I}$ (mSv $^{-1}$)
Maxwellian spectrum	2.64×10^{11}
Watt spectrum	7.27×10^9
1 MeV	6.73×10^9
2 MeV	6.67×10^9
3 MeV	6.80×10^9
4 MeV	6.86×10^9
5 MeV	6.91×10^9

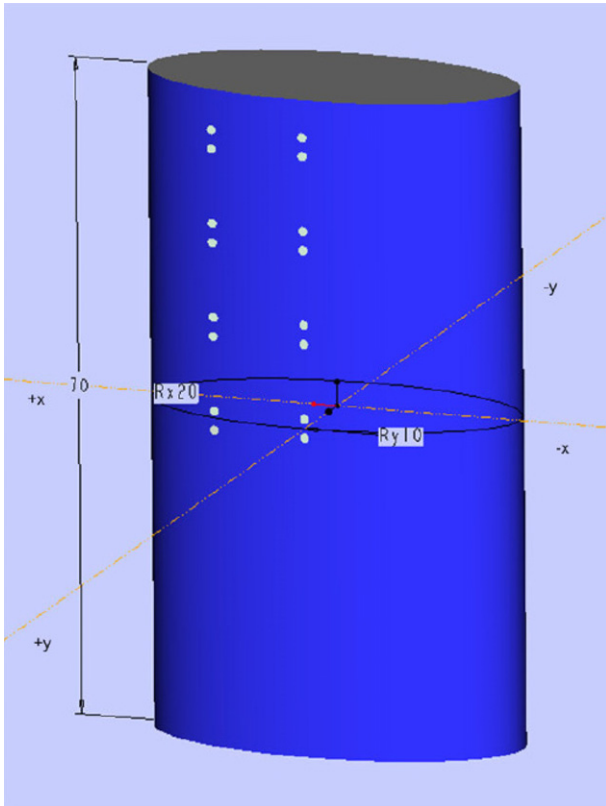


Fig. 2. Schematic showing the eight locations on the phantom surface where the detector pairs were placed.

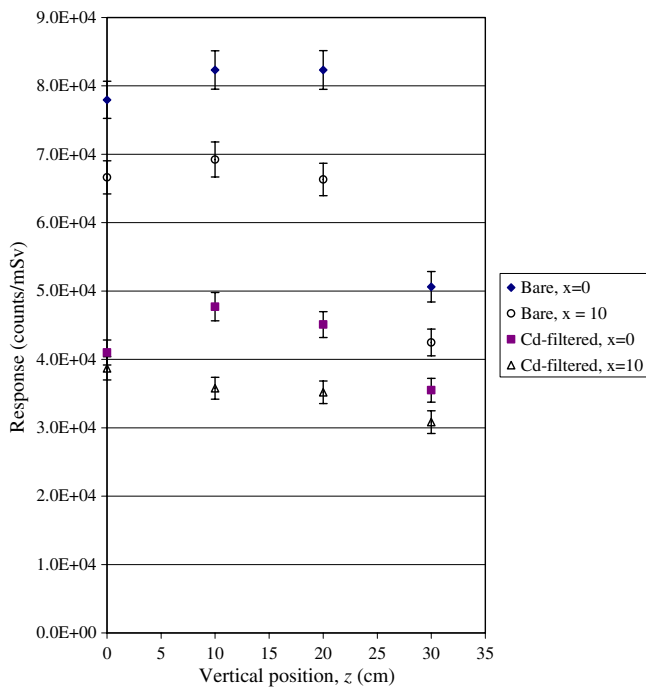


Fig. 3. Estimated detector responses for a Watt spectrum of ^{235}U fission neutrons.

the first four detector pairs were located on the front surface of the phantom at $y = 10$ cm, $x = 0$ and at vertical positions $z = 0, 10, 20$ and 30 cm, where $z = 0$ is the mid-height of the phantom. The other four detector pairs were offset to the side by 10 cm ($x = 10$ cm), were placed at $y = 8.66025$ cm and rotated by 16.1° so as to be tangent to the phantom and occupied the same four vertical positions.

We generated results for all eight positions and all seven neutron energy cases. Typical results are shown in Fig. 3 for the Watt spectrum. The variation between centered and offset positions is not large (typically within 10–20%) and the variation with vertical position is small except for the detector pair within 5 cm of the top of the phantom. This indicates that the response will not be highly dependent on where on a torso the dosimeter is placed. The detector response was of course much higher for the Maxwellian spectrum.

4. Discussion

We are constructing and testing neutron dosimeters that utilize bare and Cd-filtered semiconductor detectors that have been perforated and coated with neutron reactive material. Integrating the detectors into compact devices with micro-controller electronics will allow us to produce devices suitable for personnel dosimetry or as area monitors. The devices will be capable of near 50% efficiency, will be operable with battery power, will be insensitive to γ -ray backgrounds, will be compact and will provide real-time readout in dose equivalent or dose equivalent rate units.

Acknowledgement

This work is funded by the Department of Energy through Grant DE-FG07-04ID14599.

References

- [1] D.S. McGregor, R.T. Klann, H.K. Gersch, E. Ariesanti, J.D. Sanders, B. VanDerElzen, IEEE Trans. Nucl. Sci. 49 (2002) 1999.
- [2] V. McLane, C.L. Dunford, P.F. Rose, Neutron Cross Sections, Vol. 2, Academic Press, San Diego, CA, 1988.
- [3] J.F. Briesmeister, MCNP – A General Monte Carlo N-particle Transport Code, Los Alamos National Laboratory, LA-12625-M, Version 4C, 2000.
- [4] NCRP, Report 95, National Council on Radiation Protection and Measurements, Washington, DC, 1987.
- [5] ICRU, ICRU Report No. 66, Nuclear Technology Publishing, Kent, England, 2001.